Biology of Reproduction, 2017, 96(4), 907–920
doi:10.1093/biolre/iox010
Research Article
Advance Access Publication Date: 7 March 2017

OXFORD

Research Article

Different expression patterns of sperm motility-related genes in testis of diploid and tetraploid cyprinid fish†

Fangzhou Hu[1,2,‡], Kang Xu[1,2,‡], Yunfan Zhou[1,2,‡], Chang Wu[1,2,‡], Shi Wang[1,2], Jun Xiao[1,2], Min Wen[1,2], Rurong Zhao[1,2], Kaikun Luo[1,2], Min Tao[1,2], Wei Duan[1,2] and Shaojun Liu[1,2,*]

[1]State Key Laboratory of Developmental Biology of Freshwater Fish, Hunan Normal University, Changsha, Hunan, P. R. of China and [2]College of Life Sciences, Hunan Normal University, Changsha, Hunan, P. R. of China

*__Correspondence:__ State Key Laboratory of Developmental Biology of Freshwater Fish, Hunan Normal University,College of Life Sciences, 36 Lu Shan Road, Yue Lu District, Changsha 410081, Hunan, People's Republic of China.
E-mail: lsj@hunnu.edu.cn

†__Grant Support:__ This research was supported by National Natural Science Foundation of China Grants 30930071, 91331105, 31360514, 31430088, 31210103918 and 31272651, the Cooperative Innovation Center of Engineering and New Products for Developmental Biology of Hunan Province (20134486), the Construction Project of Key Discipline of Hunan Province and China, the National High Technology Research and Development Program of China (Grant No. 2011AA100403), Hunan Normal Unversity Graduate Research Innovation Project (CX2016B173).
‡These authors contributed equally to this work.

Received 14 December 2016; Revised 13 February 2017; Accepted 1 March 2017

Abstract

Sperm motility is an important standard to measure the fertility of male. In our previous study, we found that the diploid spermatozoa from allotetraploid hybrid (4nAT) had longer durations of rapid and slow progressive motility than haploid spermatozoa from common carp (COC). In this study, to explore sperm motility-related molecular mechanisms, we compared the testis tissues transcriptomes from 2-year-old male COC and 4nAT. The RNA-seq data revealed that 2985 genes were differentially expressed between COC and 4nAT, including 2216 upregulated and 769 downregulated genes in 4nAT. Some differentially expressed genes, such as tubulin genes, dynein, axonemal, heavy chain(dnah) genes, mitogen-activated protein kinase(mapk) genes, *tektin 4*, FOX transcription factors, proteasome genes, and ubiquitin carboxyl-terminal hydrolase(uchl) genes, are involved in the regulation of cell division, flagellar and ciliary motility, gene transcription, cytoskeleton, energy metabolism, and the ubiquitin–proteasome system, suggesting that these genes were related to sperm motility of the 4nAT. We confirmed the differential expression of 12 such genes in 4nAT by quantitative PCR. By western blotting, we also confirmed increased expression of Uchl3 in 4nAT testis. In addition, we identified 1915 and 2551 predicted long noncoding RNA (lncRNA) transcripts from testis tissue transcriptomes of COC and 4nAT, respectively. Of these, 1575 lncRNAs were specifically expressed in 4nAT and 939 were specifically expressed in COC. This study provides insights into the transcriptome profile of testis tissues from diploid and tetraploid, which are useful for research on regulatory mechanisms behind sperm motility in male polyploidy.

Summary Sentence

Clues of variations in tetraploid testis are characterized by comparative transcriptome analysis between tetraploid hybrid and common carp.

Key words: sperm motility, tetraploid hybrid, testis tissues, transcriptome, lncRNA.

Introduction

Sperm motility has been considered the main indicator of sperm quality, and it is significantly correlated with the fertilization rate [1]. As lower vertebrates, most fishes are oviparous and can undergo in vitro fertilization. The quality of the gametes plays an important role in fish genetic breeding [2]. Research on the biology of fish sperm began in the 19th century and has mainly focused on sperm morphology and structure, sperm motility, spermatogenesis, sperm metabolism, and the biochemical components of seminal plasma [3–5]. The lifespan of fish spermatozoa is affected by internal and external factors: the internal ones include gonadal development status, health condition, and age, while the external ones include osmolality, ions, carbon dioxide, and pH [6–10]. However, little is known about the mechanisms by which these factors influence sperm motility. Compared with mammals, fish spermatozoa have a shorter period of rapid and slow progressive motility (from 30 s to several minutes) after release into external medium [11, 12]. For example, the lifespan of rainbow trout spermatozoa does not exceed 60 s, while that of common carp does not exceed 120 s [13]. As such, fish spermatozoa must find an egg and complete fertilization within a short period. Thus, the fertilization rate of fish is greatly affected by the lifetime of spermatozoa.

Owing to the limited availability of material, few studies have focused on the sperm motility of polyploid fish. In our previous study, bisexual fertile allotetraploid hybrid (4nAT) populations were produced by crossing red crucian carp (*Carassius auratus* red variety) with the common carp (*Cyprinus carpio* L.) [14]. Diploid spermatozoa could be stably produced by male 4nAT, and scanning electron microscopy showed that the average head diameter of diploid spermatozoa was 2.40 μm, compared with 1.90 μm for haploid spermatozoa [14]. In addition, we found that diploid spermatozoa from 4nAT had longer durations of rapid and slow progressive motility than haploid spermatozoa from COC [15]. Thus, 4nAT are not only significant for practical applications in fish breeding, but are also beneficial for comparative study of possible molecular mechanisms related to sperm motility.

RNA-seq is a recently developed method for analyzing mRNA, small RNA, noncoding RNA, and long noncoding RNA (lncRNA) in a very high-throughput and quantitative manner. It has the advantages of being highly accurate for quantifying expression levels in specific organs or tissues and being independent of genomic sequence data. As a result, in recent years, more testis analyses have been performed using RNA-seq. For example, testis transcriptomes have been profiled by RNA-seq approaches in fish such as zebrafish [16], Nile tilapia [17], catfish [18], Southern bluefin tuna [19], guppy [20], Chinese sturgeon [21], sharpsnout seabream [22], Coilia nasus [23], and olive flounder [24]. In this way, RNA-seq has provided new insights into the molecular mechanisms underlying testis development and spermatogenesis. This approach has also shown that lncRNAs, which are longer than 200 bp, play multiple roles in the regulation of many cellular processes including spermatogenesis [25–27]. LncRNAs can regulate the expression of coding genes by epigenetic modification or induce recruitment to specific target sites, such as for DNA methylation and histone modification [28–30]. Accumulating evidence has shown that irregularities of lncRNAs in sperm could act as markers and potential therapeutic targets of male infertility [31]. The dynamic change of lncRNA expression during mouse testis postnatal development also indicated that lncRNAs might play crucial roles in mammalian testis development and spermatogenesis [32].

In this paper, we present an analysis of the transcriptomes from the mature testis of COC and 4nAT. We focused on identifying genes differentially expressed during testis development in 4nAT, relative to their levels in COC, to elucidate the molecular and genetic mechanisms that may contribute to the sperm motility of 4nAT. We also identified lncRNAs from the testis tissue transcriptomes of these two fishes as preliminary research on the difference in lncRNA expression between them.

Materials and methods

Ethics statement

Animal experimenters were certified under a professional training course for laboratory animal practitioners held by the Institute of Experimental Animals, Hunan Province, China. The fish were treated humanely following the regulations of the Administration of Affairs Concerning Experimental Animals for the Science and Technology Bureau of China.

Animal materials

Two-year-old male COC and 4nAT were collected from the Engineering Center for Polyploidy Fish Breeding of the National Education Ministry, Hunan Normal University. All of the collected fish were housed for 2 years at an appropriate school density in a 0.067-ha open pool. The water pH range was 7.0–8.5, the dissolved oxygen range was 5.0–8.0 mg/L, and the ammonia–nitrogen concentration was lower than 0.01 mg/L. The sex of each fish was determined by examining a gonad tissue slice, as described by Xiao et al [33]. The ploidy types of these fish were confirmed based on their DNA contents using a flow cytometer (cell counter analyzer; Partec), as described previously [14]. Sperm motility and head diameter were evaluated by methods described previously [15]. In addition, during the reproductive seasons, 4000 embryos (including 2000 COC and 2000 4nAT embryos) were taken at random for the examination of the fertilization rate (number of embryos at the stage of gastrula/number of eggs). For both measurable data, statistical significance was assessed using Student *t*-test. Eighteen fish (including nine COC and nine 4nAT) were chosen and euthanized using 2-phenoxyethanol (Sigma) before being dissected. The testes were removed surgically, immersed in RNA Later (Invitrogen, Carlsbad, CA, USA), and stored at −20°C for total RNA extraction. We prepared three sets of testicular RNA for biological replicates for each group. Each set of RNA consisted of pooled RNA extracted from the testicular tissue of three different individuals.

RNA isolation, cDNA library construction, and sequencing

Total RNA was isolated from testicular tissues using TRIzol reagent (Invitrogen), following the manufacturer's protocol, and cleaned using the RNeasy Mini Kit (Qiagen). The quantity and quality of total RNA were analyzed using a spectrophotometer (Nanodrop) and by gel electrophoresis. Total RNA samples with 28S:18S ratios within the range of 1.8 to 2.0 and an RNA integrity number ranging from 8.0 to 10.0 were used for further processing. After removing genomic DNA using DNase I (Fermentas, Lithuania), the construction of cDNA from 1 μg of total RNA per sample was performed following the protocol for Illumina HiSeq 2000/2500 (Illumina). To select cDNA fragments of 250–350 bp in length, the library fragments were purified with the AMPure XP system (Beckman Coulter). Next, the size-selected, adaptor-ligated cDNA was incubated with 3 μL of USER Enzyme (NEB) at 37°C for 15 min, followed by 5 min at 95°C. PCR was then performed using the Phusion High-Fidelity DNA polymerase (Thermo Scientific), Universal PCR primers (New England BioLabs), and the Index (X) Primer (New England BioLabs). PCR products were purified (AMPure XP system; Beckman Coulter) and library quality was assessed on the Agilent Bioanalyzer 2100 system (Agilent Technologies, Inc.). Clustering of the index-coded samples was then performed using a cBot Cluster Generation System with the TruSeq PE Cluster Kit v3-cBot-HS (Illumina), in accordance with the manufacturer's instructions. After cluster generation, the library preparations were sequenced on the Illumina Hiseq 2000/2500 platform and paired-end reads were generated. All of the data were deposited into the NCBI Sequence Read Archive database.

De novo assembly and gene annotation

Raw reads were filtered using the FastQC software (Babraham Bioinformatics) [34] to obtain the paired-end clean reads. All of the clean reads were used for assembly using Trinity (parameters: minimum assembled contig length to report = 100 bp; maximum length expected between fragment pairs = 250 bp; and minimum count for K-mers to be assembled by Inchworm = 4, which is specific for the de novo assembly of short reads [35, 36]. We then used the TIGR Gene Indices clustering tool TGICL (The Institute for Genomic Research, Rockville, MD; parameters: minimum overlap length = 40 bp and maximum length of unmatched overhangs = 20 bp) to remove redundant sequences and perform further assembly [37].

BLASTX alignment (e-values < 1e−5) of the above-mentioned contigs was performed using the NCBI nonredundant nucleotide database (NR), NCBI-nucleotide (NT), and Swiss-Prot as reference databases. The best alignment results were used to decide the sequence direction of contigs. The associated gene name and Gene Ontology (GO) term accession number were obtained from BLASTX alignment (e-values < 1e−6) with common carp in Ensembl BioMart [38]. WeGo software was used for analysis of the GO annotations [39].

Transcript expression levels and detection of differentially expressed transcripts

To identify differentially expressed transcripts (DETs) in the testes of COC and 4nAT, we used the CD-HIT software (Sanford-Burnham Medical Research Institute) [40] (CD-HIT-EST: sequence identity threshold = 0.9, tolerance for redundance = 5, and word length = 10) to cluster transcripts and remove redundant sequences in the transcriptomes of the two fishes with different ploidy levels; we thereby obtained reference sequence data. Then, we used BLAT (University of California Santa Cruz) [41] to align paired-end reads to these reference sequences in each transcriptome, and calculated the numbers of fragments that mapped to each reference transcript. The transcript expression level was calculated using the fragments per kilobase per million fragments mapped (FPKM) method [42]. To reduce the noise of short transcripts with lower expression, we filtered out the reference transcripts in which the FPKM was <0.07 in all samples of each group. Finally, we used DEseq [43] in R (University of Auckland) to search for DETs using a false discovery rate (FDR) of <0.001 and a threshold normalized absolute log2 fold change of ≥2.

To detect transcripts that may be related to sperm motility, we identified the transcripts that were differentially expressed in the testis of 4nAT compared with those in COC. To obtain a deeper understanding of the function of DETs in 4nAT, we investigated the biological processes and pathways in which they were enriched. The WEGO software was used to classify the GO terms of the DETs [39]; KOBAS (Center for Bioinformatics, Peking University) [44] was then used to map the DETs to KEGG pathways based on their annotation. KEGG pathways with corrected P values ≥ 0.05 were considered to be significantly enriched.

Long noncoding RNA identification

To define a set of putative lncRNAs in the transcriptomes of 4nAT and COC, we applied several filtering criteria. All of the transcripts not overlapping with fish protein-coding genes and being located at least 1 kb away from the closest annotated protein were considered for our analysis. A series of filtering steps were then implemented. The first one consisted of selecting the transcripts for which Coding Potential Calculator (CPC) [45] returned no (or just partial) coding potential. Coding–Noncoding Index (CNCI) [46] was then used to search all possible protein noncoding sequences. Similarly, RPS-Blast (NCBI Package version 2.2.25) was used to search the possible translational products of each transcript against a database of Pfam profiles [47] and the transcripts returning an expectation value lower than 10^{-5} were removed. To filter the transcripts belonging to known classes of RNAs (snoRNAs, tRNAs, etc.), all of the sequences were sought against Rfam (Release 10.0) [48] using the Rfam search facility available online (http://rfam.sanger.ac.uk/search#tabview=tab0).

Finally, the remaining transcripts were remapped against the COC genome and the homologous positions were intersected with protein-coding gene annotations (GENCODE version 3c). The screening was performed using a combination of BlastN and exonerate. The transcripts whose common carp homolog resulted to be fully included in protein-coding exons were removed.

Quantitative real-time PCR analysis

To examine the reliability of the RNA-seq results, 12 differentially expressed genes (DEGs) (*cd74*, *pank4*, *hbb*, *dnah3*, *foxk2*, *mapk4*, *tuba8l*, *ube2g1*, *psma6a*, *cfap99*, *uchl3*, *psma8a*) involved in the development of testis tissues were selected randomly for validation using quantitative real-time PCR (qPCR). The total RNAs were extracted from the remaining testicular tissue and reverse-transcribed to first-strand cDNA using reverse transcriptase (Invitrogen). The real-time PCR analysis was performed using the Prism 7500 Sequence Detection System (Applied Biosystems) with a miScript SYBR Green PCR kit (Qiagen). Real-time qPCR was performed on biological replicates in triplicate (and triplicate technical qPCR replicates).

The reaction mixture (10 μL) comprised 2.5 μL of cDNA (1:4 dilution), 5 μL of SYBR Premix Ex TaqTM II (TaKaRa), 0.5 μL of specific forward primer, 0.5 μL of universal primer, and 1.5 μL of water. The amplification conditions were as follows: 50°C for 5 min and 95°C for 10 min, followed by 40 cycles at 95°C for 15 s and 60°C for 45 s. The average threshold cycle (Ct) was calculated for each sample using the $2^{-\Delta\Delta Ct}$ method and normalized to beta-actin. Finally, a melting curve analysis was performed to validate the specific generation of the expected product. The primers used are shown in Supplemental Table S1.

Western blotting

We analyzed the conservation of some proteins encoded by the DEGs and selected one highly conserved protein, ubiquitin C-terminal hydrolase L3 (Uchl3), for which commercially available antibodies could be used, for western blotting. First, samples containing 40 μg of total lysed protein from COC and 4nAT testis were electrophoresed on a 15% SDS-PAGE gel for 1–2 h at 100 V, transferred to a polyvinylidene fluoride membrane (GE Healthcare Bio-Sciences, Uppsala, Sweden), and then blocked in TBST containing 5% nonfat milk for 1 h at room temperature. The membrane was incubated with primary antibodies (rabbit polyclonal antibody to Uchl3, 1:2000; GeneTex) overnight at 4°C. Blots were then washed extensively and incubated with the corresponding peroxidase-conjugated anti-rabbit IgG (1:5000, Sigma) for 1 h at room temperature. Proteins were detected using an ECL kit (Thermo Fisher Pierce, USA) using the ChemiDoc XRS+ imaging system (Bio-Rad, CA, USA).

Results

Transcriptome assembly and annotation

Two-year-old male COC and male 4nAT were used in this study (Figure 1A and B). The ploidy of the COC and 4nAT was determined by flow cytometry (Figure 1C and D). Many mature sperm were found in testis tissues, indicating that these two fishes with different ploidy were sexually mature (Figure 1E and F). The average sperm head diameters for diploid and allotetraploid fishes were 1.90 and 2.40 μm, respectively (Figure 1G and H). The mean durations of rapidly progressive motility were approximately 42.66 and 86.73 s for haploid spermatozoa and diploid spermatozoa, respectively; the sperm lifespan was approximately 57.54 s for the COC and 138.43 s for the 4nAT fish in distilled water. Clear differences in the duration of rapid motility and lifespan were observed between COC and 4nAT after activation ($P < 0.05$, Table 1). The average fertilization rate of 4nAT (97.8%) was higher than COC (91.2%).

The complete clean reads for these libraries have been uploaded onto the NCBI Sequence Read Archive site SRX857397, SRX699280, SRX699278 and SRX2395292. After de novo assembly, elimination of redundant sequences, and further assembly, we obtained the final transcripts for each sample from the two fishes. The final transcript data sets from the three COC samples were also pooled and assembled for subsequent analyses, as were those of the 4nAT group. The quality of assembled transcripts from the COC testis was slightly higher than that for the 4nAT testis.

Noise from short transcripts influences the results of annotation and the intuitive analysis of the data; to reduce such noise in the pooled assembled transcriptomes, we chose one representative transcriptome from each group, which was separately assembled and used for comprehensive analysis of the annotation and function of genes in the transcriptomes. The annotation revealed that 125,922 (99.7%) and 166,168 (99.0%) of the assembled transcripts in the representative COC and 4nAT transcriptomes, respectively, had at least one positive hit. Detailed annotated information is provided in Table 2.

Detection of differentially expressed transcripts

We used the Benjamini–Hochberg method [49] to detect DETs and defined an expression level of >4-fold change and FDRs of no more than 0.001 to filter genes with significant differential expression between these two fishes. A total of 2985 genes were differentially expressed between diploid and tetraploid fishes. Overall, 2216 were upregulated in tetraploid fish while 769 were downregulated, compared with their levels in the COC (Figure 2).

Functional enrichment analysis results for differentially expressed genes

The mapping of all DEGs to the terms of the GO database enabled annotation of 1176 DEGs, of which 595, 928, and 933 could be grouped into the cellular component, molecular function, and biological process categories, respectively (Figure 3). For cellular component, cell part (461, 77.48%), cell (461, 77.48%), membrane (331, 55.63%), organelle (258, 43.36%), organelle part (104, 17.48%), and extracellular region (85, 14.29%) represented the majorities of this category. Binding (606, 65.30%), catalytic activity (390, 42.03%), nucleic acid binding transcription factor activity (80, 8.67%), receptor activity (78, 8.41%), transporter activity (72, 7.76%), and enzyme regulatory activity (44, 4.74%) represented a high percentage of the molecular function category. In addition, single-organism process (610, 65.38%), cellular process (601, 65.38%), metabolic process (447, 47.91%), biological regulation (413, 44.27%), response to stimulus (281, 30.12%), developmental process (243, 26.05%), multicellular organismal process (217, 23.26%), localization (162, 17.36%), signaling (151, 16.18%), and cellular component organization or biogenesis (94, 10.08%) possessed the majorities of the biological process category.

A total of 550 DEGs were assigned to the COG classifications (Figure 4). Among the 24 COG categories, the top 15 COG categories in descending order were as follows: general function prediction (137, 24.90%), replication, recombination, and repair (65, 11.81%), signal transduction mechanisms (53, 9.64%), transcription (44, 8.00%), carbohydrate transport and metabolism (27, 4.91%), post-translational modification, protein turnover, and chaperones (26, 4.73%), amino acid transport and metabolism (25, 4.55%), cytoskeleton (22, 4.00%), cell cycle control, cell division, and chromosome partitioning (21, 3.82%), inorganic ion transport and metabolism (19, 3.45%), secondary metabolite biosynthesis, transport, and catabolism (17, 3.09%), energy production and conversion (15, 2.73%), lipid transport and metabolism (15, 2.73%), translation, ribosomal structure, and biogenesis (12, 2.18%), and function unknown (12, 2.18%).

The KEGG pathway annotation enabled us to assign 371 DEGs to 156 pathways. Pathway enrichment analysis revealed that the seven most enriched pathways were cytokine–cytokine receptor interaction (Ko04620), intestinal immune network for IgA production (Ko04672), PPAR signaling pathway (Ko03320), complement and coagulation cascades (Ko04610), arachidonic acid metabolism (Ko00590), sulfur relay system (Ko04122), and the Jak-STAT signaling pathway (Ko04630). These enriched pathways function in cell proliferation, steroidogenesis activity, receptor binding, and energy metabolism, which might confer the differences in the developmental process of testis tissues between COC and 4nAT. The top 20 most enriched pathways are shown in Figure 5.

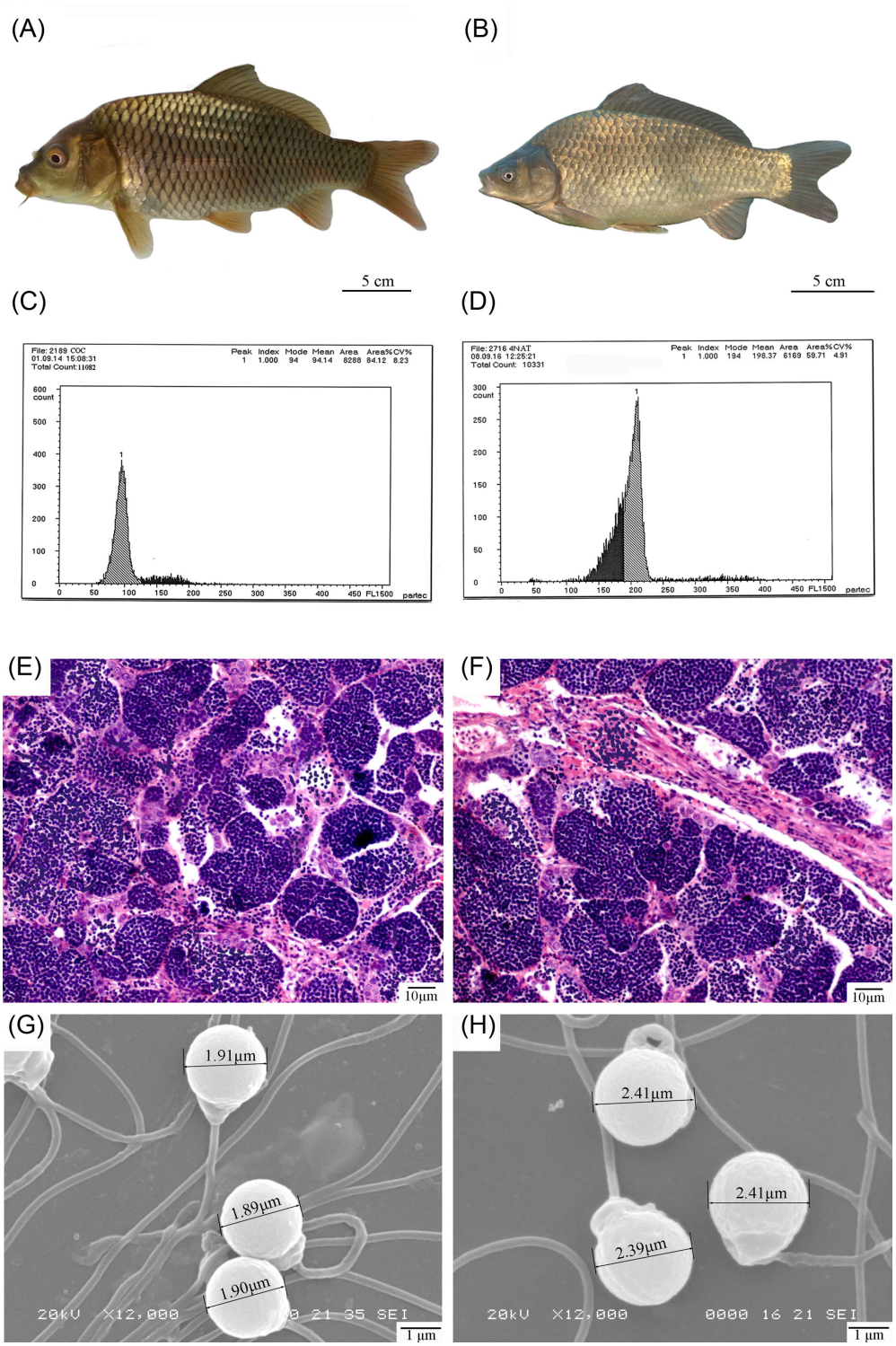

Figure 1. The appearance, DNA content, histological section of testis and structure of sperm of COC and 4nAT. The appearances of COC (A) and 4nAT (B); the DNA content of COC (C) and 4nAT (D); the testis histological section of COC (E) and 4nAT (F); the structure of sperm of COC (G) and 4nAT (H).

Long noncoding RNA identification

After a series of treatments, we eventually obtained 2551 lncRNA transcripts in 4nAT and 1915 lncRNA transcripts in COC. Of these, 1575 lncRNAs were specifically expressed in the testis of 4nAT, 939 were specifically expressed in the testis of COC, and 976 lncRNAs were expressed in both. Among these 976 coexpressed lncRNAs, 38 were differentially expressed between COC and 4nAT (Figure 6).

Table 1. The maximun velocity, initially activated ratio, fast swimming time and lifetime of haploid and diploid sperm.[a]

Sperm type	Maximum velocity (μm/s)	Fast swimming time (s)	Lifetime (s)	Initially activated sperm (%)
Diploid	135.6 ± 8.56	86.73 ± 4.76*	138.43 ± 3.12*	95.4 ± 3.6%
Haploid	130.16 ± 9.14	42.66 ± 2.32*	57.54 ± 2.31*	94.2 ± 5.4%

[a]Statistical significance was assessed using Student *t*-test.
*Showed significant difference ($P < 0.05$); no mark indicates no significant difference ($P > 0.05$).

Table 2. Detailed annotated information of representative transcriptomes in each group.

	COC	4nAT
Nr	60,312 (47.7%)	79,262 (47.2%)
Nt	125,644 (99.4%)	165,607 (98.7%)
Swiss-Prot	35,119 (27.8%)	43,747 (26.1%)
KOG	37,249 (29.5%)	46,390 (27.6%)
KEGG	21,713 (17.2%)	27,703 (16.5%)
COG	13,506 (10.7)	15,771 (9.4%)
GO	31,627 (25.3%)	40,288 (24.0%)
Pfam	35,646 (28.2%)	43,599 (26.0%)
Annotated unigenes	125,922 (99.7%)	166,168 (99.0%)
Total unigenes	126,355	167,778

Quantitative PCR validation

To validate the quality of the RNA-seq data and the reliability of genes identified to be differentially expressed in 4nAT, we chose 12 DEGs and performed qPCR on them in three biological replicates. Fold changes from qPCR were compared with the RNA-seq expression profiles (Table 3). The same trends in expression levels of these genes were detected by qPCR as were obtained from the RNA-seq data analysis (Figure 7). These results indicate the reliability of the RNA-seq data for mRNA differential expression analysis.

Western blotting

To determine whether the findings for the DEGs were reflected at the protein level, western blotting analysis with commercially available antibodies was performed in three biological replicates for the two types of fish. The data on the relative expression levels of proteins after western blotting showed that Uchl3 was more highly expressed in 4nAT testis than in COC testis (Figure 8). This result was consistent with the results of the transcriptome mRNA differential expression analysis, which partially supports the reliability of mRNA differential expression analysis.

Discussion

The testis is an important reproductive organ, and spermatogenesis plays an important role in the reproduction of most animals, including fish. To date, research on the biology of bony fish spermatozoa has mainly focused on the spermatozoon ultrastructure, sperm motility, and sperm cryopreservation [5, 50]. Tetraploidization in fish during culture is most common in cyprinids, salmonids, and catostomids [51–53]. However, there are rarely existence bisexual fertile allotetraploid fish, especially fertile male allotetraploid are difficult to produce. In our previous study, we established a stable strain of allotetraploid fish by crossing red crucian carp (female) and common carp (male) [14]. They produced stable diploid gametes and have now been propagated for 24 generations. This establishment of an artificial tetraploid lineage is of fundamental significance to evolutionary biology and genetic breeding.

In our early studies, diploid spermatozoa from 4nAT have larger heads diameter, double the DNA content and higher motility than haploid spermatozoa from COC [15]. In addition, the average fertilization rate of 4nAT was higher than COC. In this study, we used the RNA-Seq technology to present the transcriptome profiling of testis tissues from 4nAT and COC. The identified DEGs between 4nAT and COC will not only help us to understand the molecular mechanism of testis development and maturation, but also will provide valuable information for studying the DEGs related to sperm motility of fish with different types of ploidy.

Some of the DEGs identified in this study are related to sperm motility of 4nAT. These include mitogen-activated protein kinase (mapk) genes, which encode proteins that play a key role in vertebrate development, differentiation, proliferation, survival, migration, growth, and apoptosis [54, 55]. Four major MAPKs are known in mammals: extracellular signal regulated kinase (ERK), c-Jun N-terminal kinases/stress-activated protein kinases (JNK/SAPKs), p38 kinase (p38), and big MAP kinase1/extracellular signal regulated kinase 5 (BMK1/ERK5) [56–58]. EPK1/MAPKs were reported to play an important role during the meiotic progression of mouse spermatocytes [59–62] and in adhesive function at the Sertoli–germ cell interface [63]. On the other hand, MAPK is also related to motility, capacitation, and acrosome reaction in mature mammalian spermatozoa [64–66]. MAPK8 is associated with spermatids apoptosis in rats [67]. Early transcription of the *Mapk8ip1* gene is required for the survival of the fertilized oocytes in mice [68]. In this study, *mapk8a* expression was lower in the testis of 4nAT than in COC, but the *mapk8ip1* was overexpressed in the 4nAT testis. The altered expression of these genes may be directly or indirectly related to higher sperm motility in 4nAT.

Dynein, axonemal, heavy chain (dnah) genes, which encode inner dynein heavy chains that have microtubule motor activity and ATPase activity, are involved in sperm flagellar assembly, the motility of flagella, and sperm motility [69, 70]. In previous studies, mutations in the *DNAH5* and *DNAH11* were identified in patients affected by isolated asthenozoospermia [71]. In addition, loss of *Dnah1* results in male infertility and reduced ciliary beat frequency in mouse [72]. In this study, we found increased expression of *dnah2*, *dnah7*, *dnah12*, and *dnah71* in the testis of the 4nAT group compared with that in COC. The high level of these dynein genes in the 4nAT testis may thus be related to the higher sperm motility of 4nAT.

Tubulin genes form a large family, many members of which have been characterized. Tubulin is the main component of microtubules and consists of a heterodimer of alpha-tubulin and beta-tubulin; it participates in cell division, and flagellar and ciliary motility [73]. Many studies have confirmed that the tubulin expression level is related to sperm motility. For example, carbon ion irradiation was shown to induce a reduction of tubulin in the sperm of mice, which resulted in low sperm motility [74]. Similar results have been

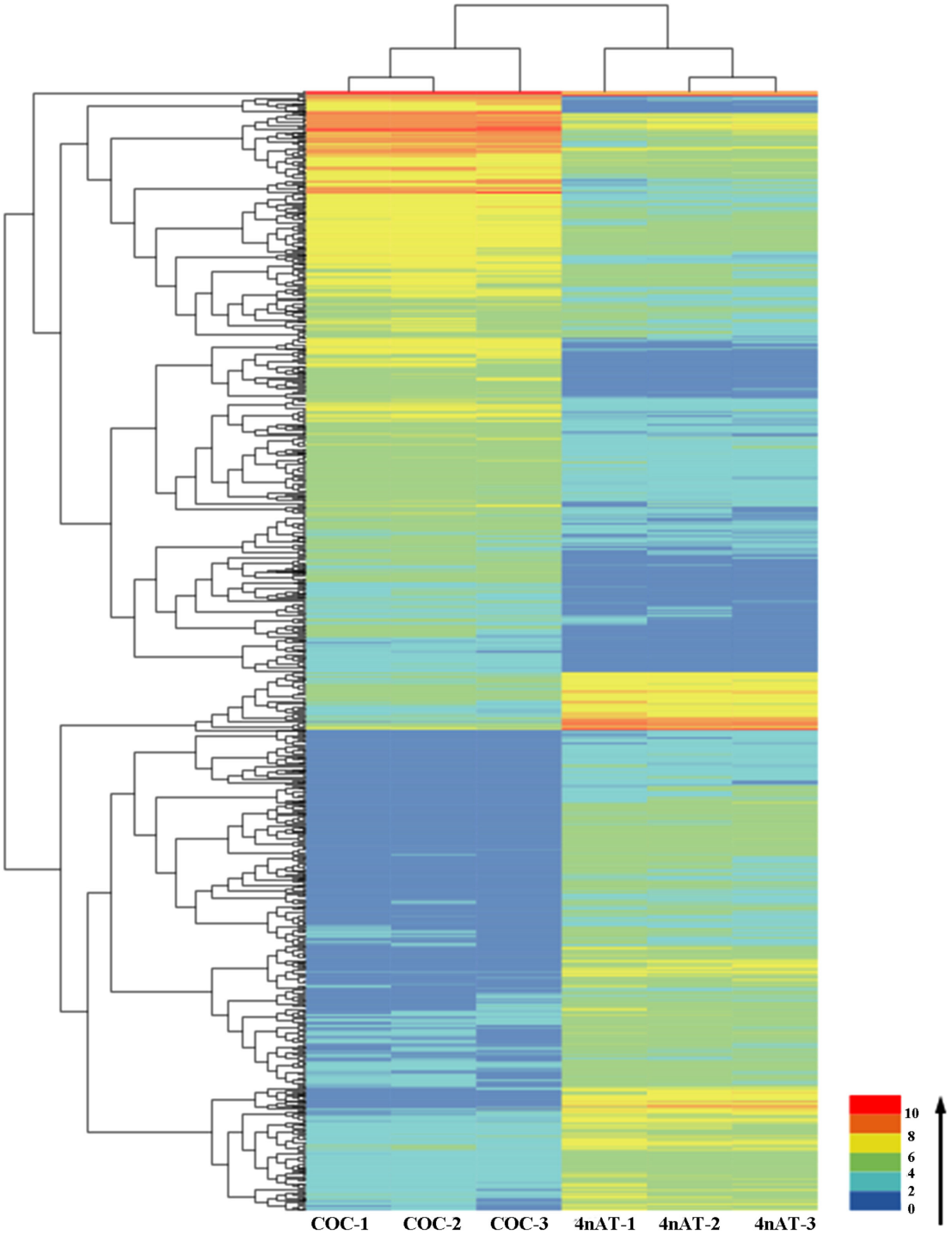

Figure 2. Hierarchical clustering analysis of the relative expression data between COC and 4nAT. In the left panel, the sample clustering aligns with two different fishes (COC/4nAT). The color scale in the right plot is dominated by small numbers and is highlighted with an arrow. "COC-1," "COC-2," and "COC-3" represent each sample from the common carp; "4nAT-1," "4nAT-2," and "4nAT-3" represent each sample from the tetraploid fish.

obtained in human studies, in that the expression level of beta-tubulin was lower in asthenozoospermic individuals than in normospermic ones [75, 76]. Tubulin gamma complex associated protein 4 (*tubgcp4*) gene encodes protein h76p which is recruited to the spindle poles and to *Xenopus* sperm basal bodies [77]. In this study, the levels of *tubb1*, *tubb2*, *tuba1b*, *tubgcp4*, and *tubd1* were higher in the testis of 4nAT than in that of COC. The high level of these tubulin family genes may be also related to the higher motility of 4nAT.

Tekt4 is a member of the Tektin gene family, which encode Tekts that are involved in the formation of sperm flagella and potentially in flagellar stability and sperm motility [78]. Previous research showed

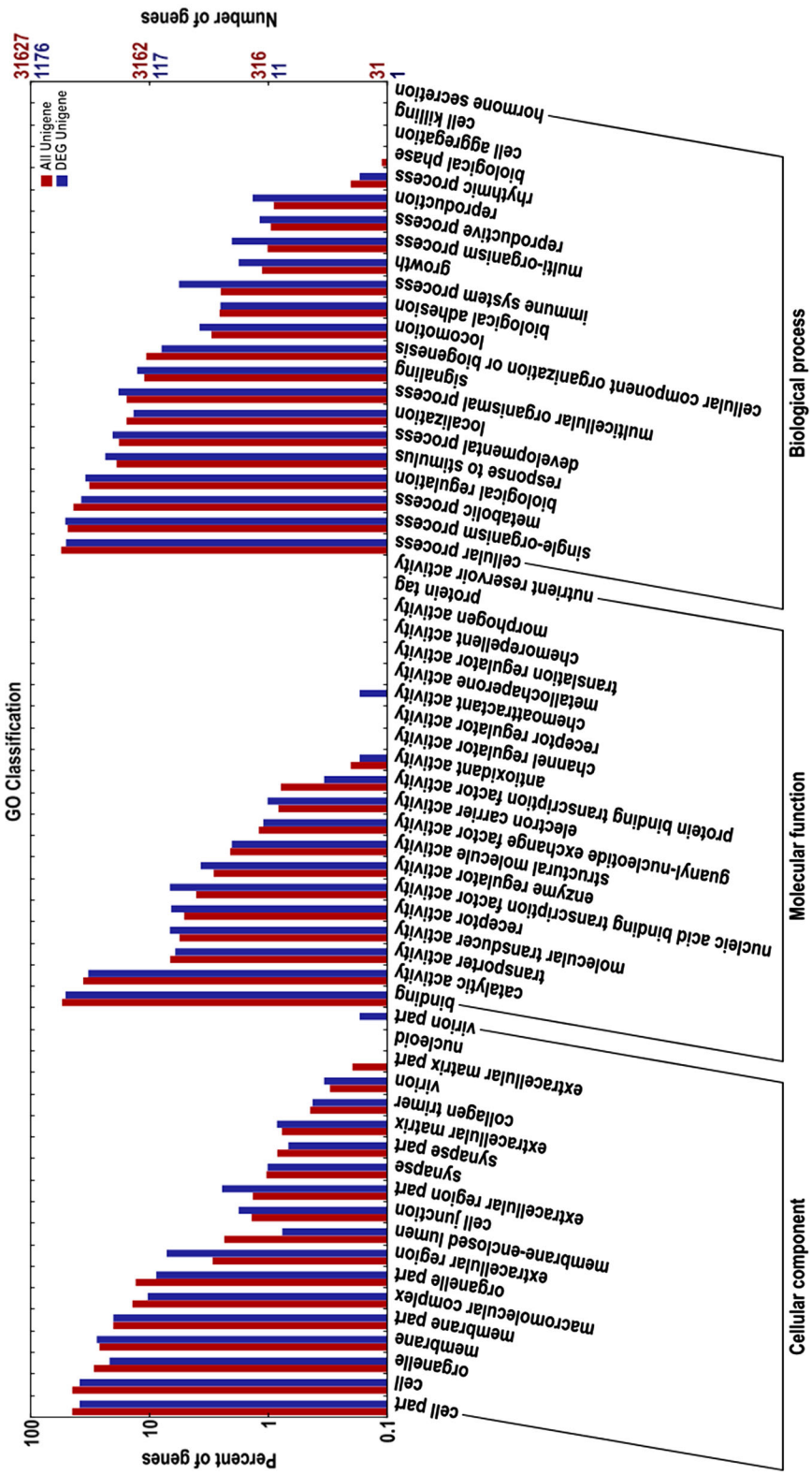

Figure 3. GO classification of the DEGs and all unigenes. Unigenes are annotated into three categories: biological process, molecular function, and cellular component. Classifications of all annotated unigenes in two representative transcriptomes in each group are shown.

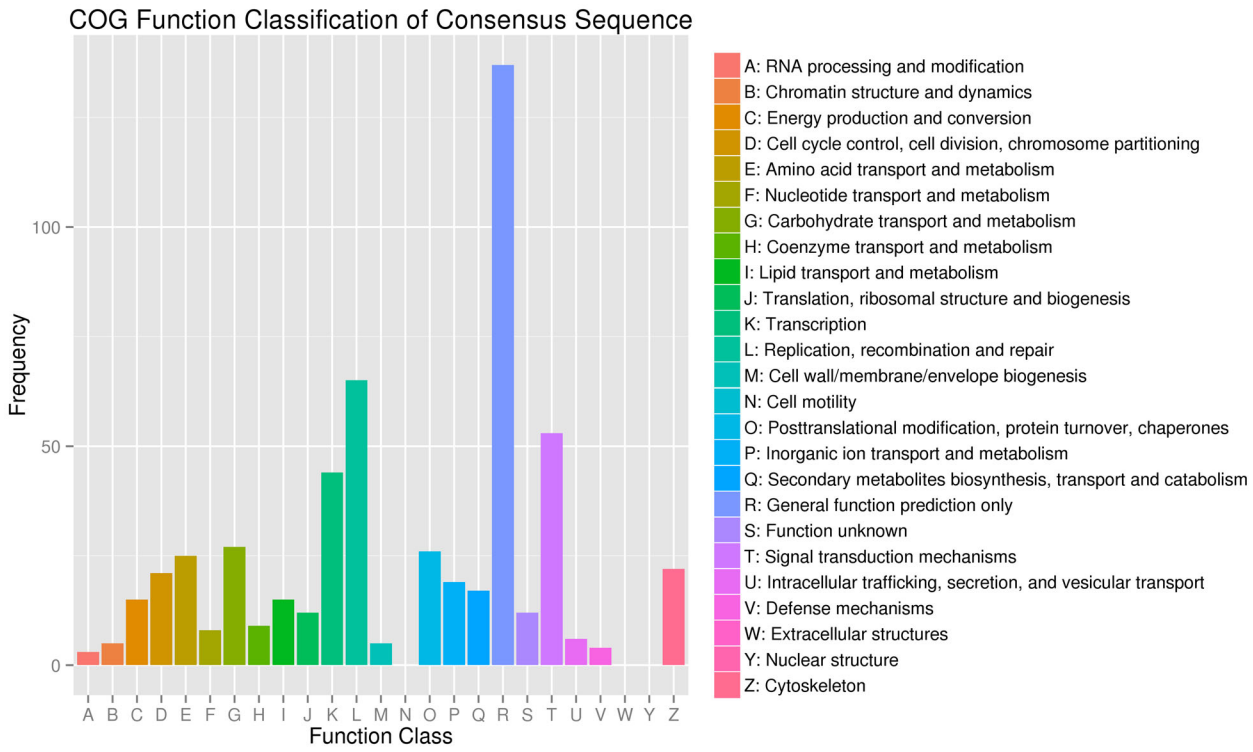

Figure 4. The COG classifications of DEGs.

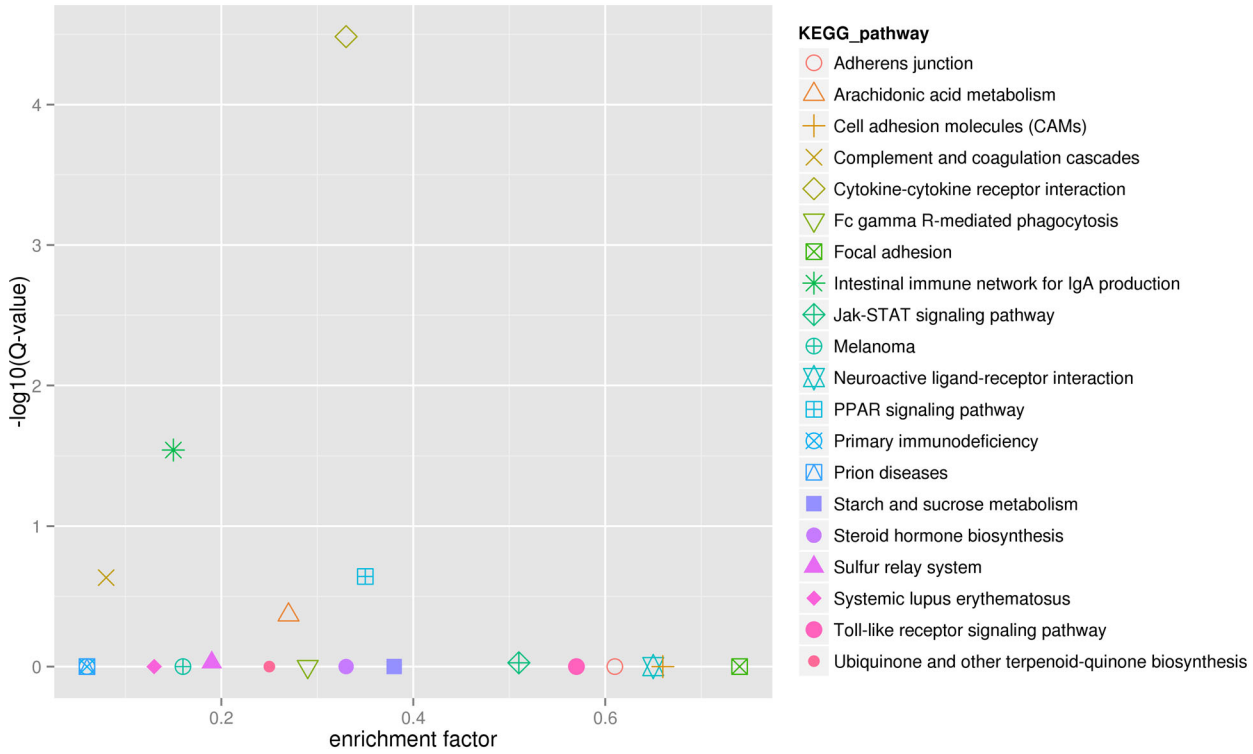

Figure 5. The top 20 most enriched pathways.

that the absence of Tekt4 causes asthenozoospermia and subfertility in male mice [79]. Similar results have been shown in human studies, namely, that the expression of *Tekt4* mRNA is significantly lower in the ejaculated sperm of idiopathic asthenozoospermia patients than in those of normozoospermic men [80]. In this study, *tekt4* was expressed at a higher level in the testis of 4nAT fish than in that of COC, also suggesting that a high level of *tekt4* expression may be related to the motile spermatozoa in 4nAT.

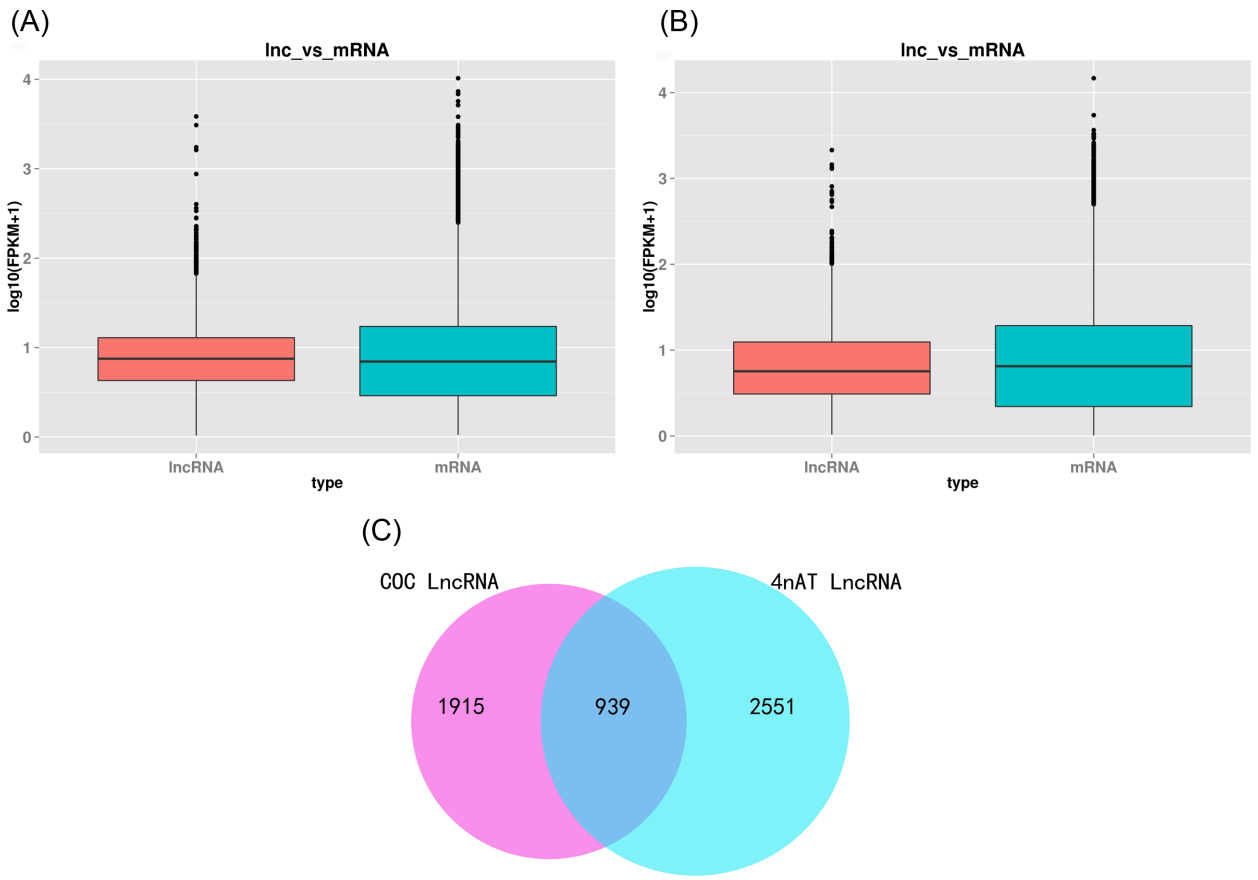

Figure 6. The distribution and relative expression of lncRNA of COC and 4nAT. (A) Boxplots of expression level (log_{10} FKPM) for annotated lncRNA and mRNA in COC. (B) Boxplots of expression level (log_{10} FKPM) for annotated lncRNA and mRNA in 4nAT. (C) The distribution of lncRNA in COC and 4nAT.

Table 3. Quantitative PCR validation of the randomly selected genes.

Item	Downregulated genes					Upregulated genes					
Gene	*tuba8l*	*dnah3*	*psma6a*	*foxk2*	*mapk4*	*psma8a*	*uchl3*	*ube2g1*	*cfap99*	*pank4*	*hbb*	*cd74*
RNA-seq	−10.7128	−5.0096	−11.1473	−4.1181	−2.2894	14.0292	13.0375	8.9203	14.4218	2.2876	3.5861	4.0304
q-pcr	−12.2807	−6.6571	−11.2919	−5.0823	−2.6323	14.3522	14.6285	7.6423	13.2987	3.1867	6.8846	3.9095

Proteasomes are large protein complexes present in all eukaryotes and archaea, and in some bacteria [81]. Proteasome activity has been detected in spermatozoa from mollusks, fish, and mammals, and is associated with mammalian sperm capacitation, fertilization, and motility [82–85]. Ubiquitin carboxyl-terminal hydrolase (UCHL) plays an important role in the processes of nerve degeneration, development of reproductive cells, and tumorigenesis of mammals. Previous studies showed that that ubiquitin–proteasome pathways exhibit significantly higher activity levels in germline tissues than in somatic tissues of Ascaris suum [86]. In carp spermatozoa, ubiquitin–proteasome pathways have also been shown to be related to sperm energy metabolism and motility [87]. In addition, in human semen, asthenozoospermic samples showed lower levels of proteasome alpha complex than those from normozoospermic patients [88]. In this study, proteasome alpha 6a subunit and 6b subunit (*psma6a* and *psma6b*) exhibited lower expression in the testis of tetraploid fish, while ubiquitin carboxyl-terminal hydrolases 1 and 3 (*uchl1* and *uchl3*) exhibited higher expression there. The different expression levels of these genes may thus also be related to the motile spermatozoa in 4nAT.

FOX transcription factors share a forkhead DNA-binding domain, and function as activators of transcription and/or as chromatin modeling factors [89–91]. A previous study showed that *FoxJ2* mRNA is expressed from the stage of pachytene spermatocytes until round spermatids, but not in spermatogonia [92]. A further study showed that FOXJ2 controls meiosis during spermatogenesis in male mice [93]. In addition, it was found that *Foxg1* transcript could be delivered from murine spermatozoa to oocytes, which plays an important regulatory role in embryo neurogenesis [94]. In this study, the forkhead family group members *foxk2*, *foxn4*, *foxg1*, and *foxh1* were overexpressed in the testis of 4nAT, which may affect the motile spermatozoa in 4nAT.

A previous study showed that coiled-coil domain-containing 42 (CCDC42) is necessary for proper sperm development and male

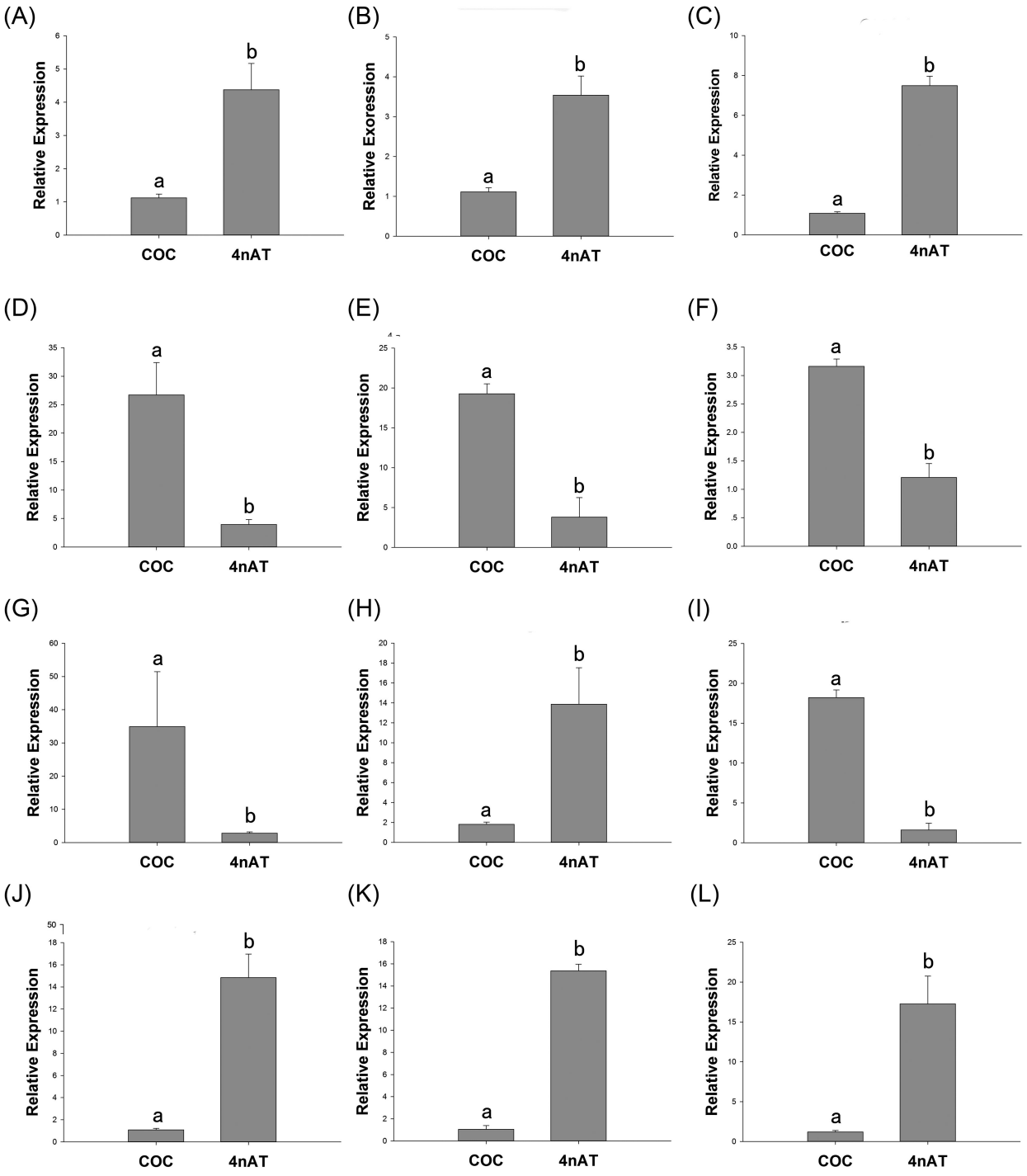

Figure 7. Real-time PCR analysis for 12 DEGs: (A) *cd74*, CD74 molecule; (B) *pank4*, pantothenate kinase 4; (C) *hbb*, hemoglobin subunit beta; (D) *dnah3*, dynein axonemal heavy chain 3; (E) *foxk2*, forkhead box K2; (F) *mapk4*, mitogen-activated protein kinase 4; (G) *tuba8l*, alpha tubulin 8 like; (H) *ube2g1*, ubiquitin conjugating enzyme E2G1 (I) *psma6a*, proteasome subunit alpha 6a; (J) *cfap99*, cilia and flagella associated protein 99; (K) *uchl3*, ubiquitin carboxyl-terminal esterase L3; (L) *psma8a*, proteasome subunit alpha 8a. In each panel, different lowercase letters indicate significant differences ($P < 0.05$) (means ± SD of relative expression; n = 9 for each group).

fertility in mouse [95]. The *Ccdc70* gene is highly expressed in mouse testis and involved in the regulation of spermatogenesis and epididymal sperm maturation [96]. Other studies have shown that CCDC125 controls cell motility through the regulation of RhoA, Rac1, and Cdc42 activity [97]. A proteomic analysis of bovine sperm cells also showed that CCDC113 is a component of centriolar satellites, which are highly conserved and function in cilium formation [98]. In this study, the coiled-coil domain-containing gene family members *ccdc42*, *ccdc125*, *ccdc149a*, *ccdc50*, *ccdc64*, *ccdc92*, and *ccdc74b* were overexpressed in the testis of tetraploid fish, but *ccdc*

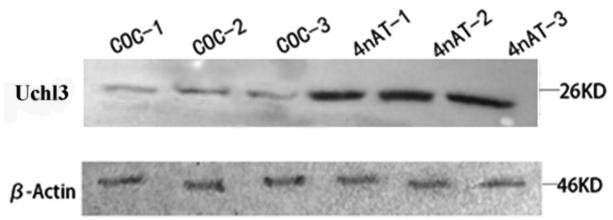

Figure 8. Verification of the expression of Uchl3 protein by western blot analysis. The total proteins were separated by 15% SDS-PAGE and transferred to PVDF membrane. "COC-1", "COC-2," and "COC-3" represent the bands from the common carp; "4nAT-1", "4nAT-2," and "4nAT-3" represent the bands from the tetraploid hybrid.

96 and *ccdc113* showed lower expression there, with both of these groups of genes being related to cilium assembly.

Long noncoding RNAs have been reported to play key roles in many cellular processes including spermatogenesis [26, 27]. For example, low lncRNA HOTAIR expression is associated with the downregulation of Nrf2 in the spermatozoa of patients with asthenozoospermia or oligoasthenozoospermia [99]. In addition, lncRNA meiotic recombination hotspot locus (*Mrhl*), *HongrES2*, testis-specific X-linked (*Tsx*), Dmrt1-related gene (*Dmr*), and Spga-lncRNAs have been reported to be involved in the regulation of spermatogenesis [31]. In this study, we preliminarily identified 1575 lncRNAs that were specifically expressed in the testis of 4nAT and 939 lncRNA transcripts that were specifically expressed in the testis of COC. In addition, we identified 12 upregulated and 26 downregulated lncRNAs in 4nAT, whose specificity and differential expression might be related to the motile spermatozoa in 4nAT.

This is the first report on the testis transcriptome of diploid and tetraploid cyprinid fishes. Functional analyses of DETs revealed some genes related to sperm motility in 4nAT, which do not act independently but instead influence biological processes through networks of interactions. Our results provide a foundation for the further characterization of gene expression during spermatogenesis in tetraploid cyprinid fish.

Supplementary data

Supplementary data are available at *BIOLRE* online.

Supplemental Table S1. The primers sequences and the products sizes of q-pcr.

Reference

1. Vladiĉ T, Jarvi T. Sperm motility and fertilization time span in Atlantic salmon and brown trout—the effect of water temperature. *J Fish Biol* 2005; **50**:1088–1093.
2. Deng YS, Lin HR. Advance in fishes sperm motility. *Life Sci Res* 1999; **3**:271–278.
3. Fribourgh JH, Soloff BL. Scanning electron microscopy of the rainbow trout (Salmo gairdneri Richardson) spermatozoon. Arkansas *Acad. Sci. Proc.* 1976; **30**:41–43.
4. Lahnsteiner F. Characterization of seminal plasma proteins stabilizing the sperm viability in rainbow trout (Oncorhynchus mykiss). *Animal Reprod Sci* 2007; **97**:151–164.
5. Billard R, Cosson MP. Some problems related to the assessment of sperm motility in freshwater fish. *J Exp Zool* 1992; **261**:122–131.
6. Cosson J. The ionic and osmotic factors controlling motility of fish spermatozoa. *Aquacult Int* 2004; **12**:69–85.
7. Morisawa M. Initiation mechanism of sperm motility at spawning in teleosts. *Zoologicalence* 1985; **2**:605–615.
8. Morisawa M, Suzuki K, Morisawa S. Effects of potassium and osmolality on spermatozoan motility of salmonid fishes. *J Exp Biol* 1983; **107**:105.
9. Morisawa M, Suzuki K. Osmolality and potassium ion: their roles in initiation of sperm motility in teleosts. *Science* 1980; **210**:1145–1147.
10. Alavi SMH, Cosson J. Sperm motility in fishes. (II) Effects of ions and osmolality: a review. *Cell Biol Int* 2006; **30**:1–14.
11. Scott AP, Baynes SM. A review of the biology, handling storage of salmonid spermatozoa. *J Fish Biol* 2006; **17**:707–739.
12. Billard R. Changes in structure and fertilizing ability of marine and preshwater fish spermatozoa diluted in media of various salinities. *Aquaculture* 1978; **14**:187–198.
13. Streitjr DP, Sirol RN, Ribeiro RP, Moraes GV, Vargas LD, Watanabe AL. Qualitative parameters of the piapara semen (Leporinus elongatus Valenciennes, 1850). *Braz J Biol* 2008; **68**:373–377.
14. Liu S, Liu Y, Zhou G, Zhang X, Luo C, Feng H, He X, Zhu G, Yang H. The formation of tetraploid stocks of red crucian carp× common carp hybrids as an effect of interspecific hybridization. *Aquaculture* 2001; **192**:171–186.
15. Duan W, Xu K, Hu F, Zhang Y, Wen M, Wang J, Tao M, Luo K, Zhao R, Qin Q. Comparative proteomic, physiological, morphological and biochemical analyses reveal the characteristics of the diploid spermatozoa of allotetraploid hybrids of Carassius auratus and common carp (Cyprinus carpio). *Biol Reprod* 2016; **94**:35.
16. Li Y, Chia JM, Bartfai R, Christoffels A, Yue GH, Ding K, Ho MY, Hill JA, Stupka E, Orban L. Comparative analysis of the testis and ovary transcriptomes in zebrafish by combining experimental and computational tools. *Comp Funct Genomics* 2004; **5**:403–418.
17. Tao W, Yuan J, Zhou L, Sun L, Sun Y, Yang S, Li M, Zeng S, Huang B, Wang D. Characterization of gonadal transcriptomes from Nile Tilapia (Oreochromis niloticus) reveals differentially expressed genes. *PLoS One* 2013; **4778**:1–10.
18. Sun F, Liu S, Gao X, Jiang Y, Perera D, Wang X, Li C, Sun L, Zhang J, Kaltenboeck L. Male-biased genes in catfish as revealed by RNA-Seq analysis of the testis transcriptome. *PLoS One* 2013; **8**:65–65.
19. Bar I, Cummins S, Elizur A. Transcriptome analysis reveals differentially expressed genes associated with germ cell and gonad development in the Southern bluefin tuna (Thunnus maccoyii). *BMC Genomics* 2016; **17**:217.
20. Sharma E, Künstner A, Fraser BA, Zipprich G, Kottler VA, Henz SR, Weigel D, Dreyer C. Transcriptome assemblies for studying sex-biased gene expression in the guppy, Poecilia reticulata. *BMC Genomics* 2014; **15**:639–650.
21. Yue H, Li C, Du H, Zhang S, Wei Q. Sequencing and de novo assembly of the gonadal transcriptome of the endangered chinese sturgeon (Acipenser 615 sinensis). *PLoS One* 2015; **10**:e0127332.
22. Manousaki T, Tsakogiannis A, Lagnel J, Sarropoulou E, Xiang JZ, Papandroulakis N, Mylonas CC, Tsigenopoulos CS. The sex-specific transcriptome of the hermaphrodite sparid sharpsnout seabream (Diplodus puntazzo). *BMC Genomics* 2014; **15**:1–16.
23. Zhou YF, Duan JR, Liu K, Xu DP, Zhang MY, Fang DA, Xu P. Testes transcriptome profiles of the anadromous fish Coilia nasus during the onset of spermatogenesis. *Marine Genomics* 2015; **24**:241–243.
24. Wei Z, Liu Y, Yu H, Du X, Zhang Q, Wang X, Yan H. Transcriptome analysis of the gonads of olive flounder (Paralichthys olivaceus). *Fish Physiol Biochem* 2016; **42**:1581–1594.
25. Mercer TR, Dinger ME, Mattick JS. Long non-coding RNAs: insights into functions. *Nat Rev Genet* 2009; **10**:155–159.
26. Caley DP, Pink RC, Trujillano D, Carter DR. Long noncoding RNAs, chromatin, and development. *Thescientificworldjournal* 2010; **10**:90–102.
27. Liang M, Li W, Tian H, Hu T, Wang L, Lin Y, Li Y, Huang H, Sun F. Sequential expression of long noncoding RNA as mRNA gene expression in specific stages of mouse spermatogenesis. *Sci Rep* 2014; **4**:5966–5966.
28. Berghoff EG, Clark MF, Chen S, Cajigas I, Leib DE, Kohtz JD. Evf2 (Dlx6as) lncRNA regulates ultraconserved enhancer methylation and the differential transcriptional control of adjacent genes. *Development* 2013; **140**:4407–4416.

29. Yap KL, Li S, Muñoz-Cabello AM, Raguz S, Lei Z, Mujtaba S, Gil J, Walsh MJ, Zhou MM. Molecular interplay of the noncoding RNA ANRIL and methylated histone H3 lysine 27 by polycomb CBX7 in transcriptional silencing of INK4a. *Mol Cell* 2010; **38**:662–674.
30. Klattenhoff C, Scheuermann J, Surface L, Bradley R, Fields P, Steinhauser M, Ding H, Butty V, Torrey L, Haas S. Braveheart , a long noncoding RNA required for cardiovascular lineage commitment. *Cell* 2013; **152**:570–583.
31. Luk AC, Chan WY, Rennert OM, Lee TL. Long noncoding RNAs in spermatogenesis: insights from recent high-throughput transcriptome studies. *Reproduction* 2014; **147**:R131–R141.
32. Sun J, Lin Y, Wu J. Long non-coding RNA expression profiling of mouse testis during postnatal development. *PLoS One* 2013; **8**:e75750.
33. Xiao J, Kang X, Xie L, Qin Q, He Z, Hu F, Zhang C, Zhao R, Wang J, Luo K. The fertility of the hybrid lineage derived from female Megalobrama amblycephala× male Culter alburnus. *Anim Reprod Sci* 2014; **151**: 61–70.
34. Andrews S. FastQC: a quality control tool for high throughput sequence data. [Internet]. Cambridge, UK: Babraham Bioinformatics, The Babraham Institute. http://www.bioinformatics.bbsrc.ac.uk/projects/fastqc/. Accessed 12 September 2011.
35. Haas BJ, Papanicolaou A, Yassour M, Grabherr M, Blood PD, Bowden J, Couger MB, Eccles D, Li B, Lieber M. De novo transcript sequence reconstruction from RNA-seq using the Trinity platform for reference generation and analysis. *Nat Protoc* 2013; **8**:1494–1512.
36. Grabherr MG, Haas BJ, Yassour M, Levin JZ, Thompson DA, Amit I, Adiconis X, Fan L, Raychowdhury R, Zeng Q. Full-length transcriptome assembly from RNA-Seq data without a reference genome. *Nat Biotechnol* 2011; **29**:644–652.
37. Pertea G, Huang X, Liang F, Antonescu V, Sultana R, Karamycheva S, Lee Y, White J, Cheung F, Parvizi B. TIGR Gene Indices clustering tools (TGICL): a software system for fast clustering of large EST datasets. *Bioinformatics* 2003; **19**:651–652.
38. Flicek P, Amode MR, Barrell D, Beal K, Billis K, Brent S, Carvalho-Silva D, Clapham P, Coates G, Fitzgerald S. Ensembl 2014. *Nucleic Acids Res* 2014; **42**:D749–D755.
39. Ye J, Fang L, Zheng H, Zhang Y, Chen J, Zhang Z, Wang J, Li S, Li R, Bolund L. WEGO: a web tool for plotting GO annotations. *Nucleic Acids Res* 2006; **34**:W293–W297.
40. Li W, Godzik A. Cd-hit: a fast program for clustering and comparing large sets of protein or nucleotide sequences. *Bioinformatics*. 2006; **22**:1658–1659.
41. Kent WJ. BLAT—the BLAST-like alignment tool. *Genome Res* 2002; **12**:656–664.
42. Mortazavi A, Williams BA, McCue K, Schaeffer L, Wold B. Mapping and quantifying mammalian transcriptomes by RNA-Seq. *Nat Methods* 2008; **5**:621–628.
43. Anders S, Huber W. Differential expression analysis for sequence count data. *Genome Biol* 2010; **11**:R106.
44. Xie C, Mao X, Huang J, Ding Y, Wu J, Dong S, Kong L, Gao G, Li C-Y, Wei L. KOBAS 2.0: a web server for annotation and identification of enriched pathways and diseases. *Nucleic Acids Res* 2011; **39**:W316–W322.
45. Kong L, Zhang Y, Ye Z-Q, Liu X-Q, Zhao S-Q, Wei L, Gao G. CPC: assess the protein-coding potential of transcripts using sequence features and support vector machine. *Nucleic Acids Res* 2007; **35**:W345–W349.
46. Sun L, Luo H, Bu D, Zhao G, Yu K, Zhang C, Liu Y, Chen R, Zhao Y. Utilizing sequence intrinsic composition to classify protein-coding and long non-coding transcripts. *Nucleic Acids Res* 2013; **41**:e166.
47. Bateman A, Coin L, Durbin R, Finn RD, Hollich V, Griffiths- Jones S, Khanna A, Marshall, M, Moxon, S, Sonnhammer EL. The Pfam protein families database. *Nucleic Acids Res* 2004; **32**:D138–D141.
48. Gardner PP, Daub J, Tate JG, Nawrocki EP, Kolbe DL, Lindgreen S, Wilkinson AC, Finn RD, Griffiths-Jones S, Eddy SR. Rfam: updates to the RNA families database. *Nucleic Acids Res* 2009; **37**:D136–D140.
49. Benjamini Y, Hochberg Y. Controlling the false discovery rate: a practical and powerful approach to multiple testing. *J Roy Stat Soc B* 1995; **57**:289–300.
50. Alavi SMH, Cosson J. Sperm motility in fishes. I. Effects of temperature and pH: a review. *Cell Biol Int* 2005; **29**:101–110.
51. Salaneck E, Larsson T, Larson ET, Larhammar D. Birth and death of neuropeptide Y receptor genes in relation to the teleost fish tetraploidization. *Gene* 2008; **409**:61–71.
52. Vasil'ev VP. Mechanisms of polyploid evolution in fish: polyploidy in sturgeons. In: *Biology, conservation and sustainable development of sturgeons. Fish and Fisheries Series* 2009; **29**:97–117.
53. Liu S. Distant hybridization leads to different ploidy fishes. *Sci China Life Sci* 2010; **53**:416–425.
54. Neill JD, Duck WL, Sellers JC, Musgrove LC, Kehrl JH. A regulator of G Protein signaling, RGS3, inhibits gonadotropin-releasing hormone (GnRH)-stimulated luteinizing hormone (LH) secretion. *BMC Cell Biol* 2001; **2**:1–10.
55. Netiv E, Liscovitch M, Naor Z. Delayed activation of phospholipase D by gonadotropin-releasing hormone in a clonal pituitary gonadotrope cell line (αT3-1). *FEBS Lett* 1991; **295**:107–109.
56. Seger R, Krebs EG. The MAPK signaling cascade. *FASEB J* 1995; **9**:726–735.
57. Gutkind JS. The pathways connecting G protein-coupled receptors to the nucleus through divergent mitogen-activated protein kinase cascades. *J Biol Chem* 1998; **273**:1839–1842.
58. Pearson G, Robinson F, Beers GT, Xu BE, Karandikar M, Berman K, Cobb MH. Mitogen-activated protein (MAP) kinase pathways: regulation and physiological functions. *Endocr Rev* 2001; **22**:732–737.
59. Sette C, Barchi M, Bianchini A, Conti M, Rossi P, Geremia R. Activation of the mitogen-activated protein kinase ERK1 during meiotic progression of mouse pachytene spermatocytes. *J Biol Chem* 1999; **274**:33571–33579.
60. Lu Q, Sun Q, Breitbart H, Chen D. Expression and phosphorylation of mitogen-activated protein kinases during spermatogenesis and epididymal sperm maturation in mice. *Arch Androl* 1999; **43**:55–66.
61. Rhee K, Wolgemuth DJ. The NIMA-related kinase 2, Nek2, is expressed in specific stages of the meiotic cell cycle and associates with meiotic chromosomes. *Development* 1997; **124**:2167–2177.
62. Di Agostino S, Botti F, Di Carlo A, Sette C, Geremia R. Meiotic progression of isolated mouse spermatocytes under simulated microgravity. *Reproduction* 2004; **128**:25–32.
63. Wong CH, Cheng CY. Mitogen-activated protein kinases, adherens junction dynamics, and spermatogenesis: a review of recent data. *Dev Biol* 2005; **286**:1–15.
64. Baldi E, Luconi M, Bonaccorsi L, Forti G. Nongenomic effects of progesterone on spermatozoa: mechanisms of signal transduction and clinical implications. *Pediatr Pathol Mol Med* 1998; **18**:417–431.
65. De Lamirande E, Gagnon C. The extracellular signal-regulated kinase (ERK) pathway is involved in human sperm function and modulated by the superoxide anion. *Mol Human Reprod* 2002; **8**:124–135.
66. Du Plessis S, Page C, Franken D. Extracellular signal-regulated kinase activation involved in human sperm-zona pellucida binding. *Andrologia* 2002; **34**:55–59.
67. Show MD, Hill CM, Anway MD, Wright WW, Zirkin BR. Phosphorylation of mitogen-activated protein kinase 8 (MAPK8) is associated with germ cell apoptosis and redistribution of the Bcl2-modifying factor (BMF). *J Androl* 2008; **29**:338–344.
68. Thompson NA, Haefliger J-A, Senn A, Tawadros T, Magara F, Ledermann B, Nicod P, Waeber G. Islet-brain1/JNK-interacting protein-1 is required for early embryogenesis in mice. *J Biol Chem* 2001; **276**:27745–27748.
69. Mattéi MG. Identification, tissue specific expression, and chromosomal localisation of several human dynein heavy chain genes. *Eur J Hum Genet* 2000; **8**:923–932.
70. Rashid S, Breckle R, Hupe M, Geisler S, Doerwald N, Neesen J. The murine Dnali1 gene encodes a flagellar protein that interacts with the cytoplasmic dynein heavy chain 1. *Mol Reprod Dev* 2006; **73**: 784–794.
71. Zuccarello D, Ferlin A, Cazzadore C, Pepe A, Garolla A, Moretti A, Cordeschi G, Francavilla S, Foresta C. Mutations in dynein genes in patients affected by isolated non-syndromic asthenozoospermia. *Hum Reprod* 2008; **23**:1957–1962.

72. Neesen J, Kirschner R, Ochs M, Schmiedl A, Habermann B, Mueller C, Holstein AF, Nuesslein T, Adham I, Engel W. Disruption of an inner arm dynein heavy chain gene results in asthenozoospermia and reduced ciliary beat frequency. *Hum Mol Genet* 2001; **10**:1117–1128.
73. McKean PG, Vaughan S, Gull K. The extended tubulin superfamily. *J Cell Sci* 2001; **114**:2723–2733.
74. Hong Yan LI, Yu Xuan HE, Zhang H, Liu YY, Miao GY, Zhao QY. Carbon ion irradiation induces reduction of β-tubulin in sperm of pubertal mice. *Biomed Environ Sci* 2014; **27**:130–133.
75. Shen S, Wang J, Liang J, He D. Comparative proteomic study between human normal motility sperm and idiopathic asthenozoospermia. *World J Urol* 2013; **31**:1395–1401.
76. Peknicova J, Pexidrova M, Kubatova A, Koubek P, Tepla O, Sulimenko T, Draber P. Expression of beta-tubulin epitope in human sperm with pathological spermiogram. *Fertil Steril* 2007; **88**:1120–1128.
77. Fava F, Raynaudmessina B, Leungtack J, Mazzolini L, Li M, Guillemot JC, Cachot D, Tollon Y, Ferrara P, Wright M. Human 76p A new member of the γ-tubulin-associated protein family. *J Cell Biol* 1999; **147**:857–868.
78. Amos LA. The tektin family of microtubule-stabilizing proteins. *Genome Biol* 2008; **9**:73–78.
79. Roy A, Lin YN, Agno JE, Demayo FJ, Matzuk MM. Absence of tektin 4 causes asthenozoospermia and subfertility in male mice. *FASEB J* 2007; **21**:1013–1025.
80. Wen-Bin WU, Yu-Shan LI, Xiao-Fei JI, Wang QX, Gao XM, Yang XF, Pan ZH. Expression of TEKT4 protein decreases in the ejaculated spermatozoa of idiopathic asthenozoospermic men. *Natl J Androl* 2012; **18**:514–517.
81. Peters JM, Franke WW, Kleinschmidt JA. Distinct 19 S and 20 S subcomplexes of the 26 S proteasome and their distribution in the nucleus and the cytoplasm. *J Biol Chem* 1994; **269**:7709–7718.
82. Pizarro E, Pastén C, Kong M, Morales P. Proteasomal activity in mammalian spermatozoa. *Mol Reprod Dev* 2004; **69**:87–93.
83. Wójcik C, Demartino GN. Intracellular localization of proteasomes. *Int J Biochem Cell Biol* 2003; **35**:579–589.
84. Inaba K, Morisawa S, Morisawa M. Proteasomes regulate the motility of salmonid fish sperm through modulation of cAMP-dependent phosphorylation of an outer arm dynein light chain. *J Cell Sci* 1998; **111** (pt 8):1105–1115.
85. Kong M, Diaz E, Morales P. Participation of the human sperm proteasome in the capacitation process and its regulation by protein kinase A and tyrosine kinase. *Biol Reprod*. 2009; **80**:1026–1035.
86. Ma X, Zhu Y, Li C, Shang Y, Meng F, Chen S, Long M. Comparative transcriptome sequencing of germline and somatic tissues of the Ascaris suum gonad. *BMC Genomics* 2010; **12**:1–11.
87. Dietrich M, Dietrich GJ, Mostek A, Ciereszko A. Motility of carp spermatozoa is associated with profound changes in the sperm proteome. *J Proteomics* 2016; **138**:124–135.
88. Siva AB, Kameshwari DB, Singh V, Pavani K, Sundaram CS, Rangaraj N, Deenadayal M, Shivaji S. Proteomics-based study on asthenozoospermia: differential expression of proteasome alpha complex. *Mol Hum Reprod* 2010; **16**:452–462.
89. Gómez-Ferrería MA, Rey-Campos J. Functional domains of FOXJ2. *J Mol Biol* 2003; **329**:631–644.
90. Granadino B, Perezsanchez C, Reycampos J. Fork head transcription factors. *Curr Genomics* 2000; **1**:353–382.
91. Kaufmann E, Knöchel W. Five years on the wings of fork head. *Mech Dev* 1996; **57**:3–20.
92. Granadino B, Ariasdelafuente C, Pérezsánchez C, Párraga M, Lópezfernández LA, Del MJ, Reycampos J. Fhx (Foxj2) expression is activated during spermatogenesis and very early in embryonic development. *Mech Dev* 2000; **97**:157–160.
93. Miao H, Miao CX, Li N, Han J. FOXJ2 controls meiosis during spermatogenesis in male mice. *Mol Reprod Dev* 2016; **83**:684–691.
94. Fang P, Zeng P, Wang Z, Liu M, Xu W, Dai J, Zhao X, Zhang D, Liang D, Chen X. Estimated diversity of messenger RNAs in each murine spermatozoa and their potential function during early zygotic development. *Biol Reprod* 2014; **90**:94–94.
95. Pasek RC, Malarkey E, Berbari NF, Sharma N, Kesterson RA, Tres LL, Kierszenbaum AL, Yoder BK. Coiled-coil domain containing 42 (Ccdc42) is necessary for proper sperm development and male fertility in the mouse. *Dev Biol* 2016; **412**:208–218.
96. Chen JB, Zheng WZ, Li YC, Lin SR, Zhang Z, Wu Y, Jiang ZM, Gui YT. Expression characteristics of the Ccdc70 gene in the mouse testis during spermatogenesis. *Zhonghua Nan ke Xue = Natl J Androl* 2016; **22**: 12–16.
97. Araya N, Arimura H, Kawahara K, Yagishita N, Ishida J, Fujii R, Aratani S, Fujita H, Sato T, Yamano Y. Role of Kenae/CCDC125 in cell motility through the deregulation of RhoGTPase. *Int J Mol Med* 2009; **24**: 605–611.
98. Firatkaralar EN, Sante J, Elliott S, Stearns T. Proteomic analysis of mammalian sperm cells identifies new components of the centrosome. *J Cell Sci* 2014; **127**:4128–4133.
99. Zhang L, Liu Z, Li X, Zhang P, Wang J, Zhu D, Chen X, Ye L. Low long non-coding RNA HOTAIR expression is associated with down-regulation of Nrf2 in the spermatozoa of patients with asthenozoospermia or oligoasthenozoospermia. *Int J Clin Exp Pathol* 2015; **8**: 14198–14205.